A geometrically flexible conservative semi-Lagrangian scheme for multi-tracer transport

Peter Hjort Lauritzen

Atmospheric Modeling & Predictability Section
Climate & Global Dynamics Division
National Center for Atmospheric Research, Boulder, Colorado


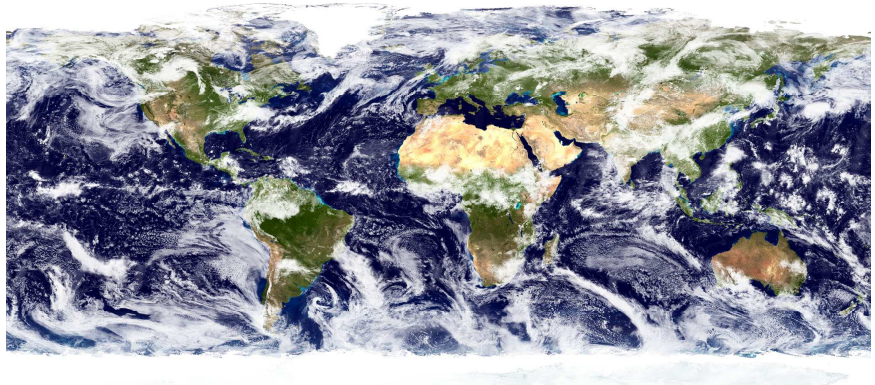


Workshop II: Model and Data Hierarchies for Simulating and Understanding Climate
Institute for Pure and Applied Mathematics (IPAM)
University of California Los Angeles (UCLA)

1. Motivation: Why focus on tracer transport? (context: global climate models)
   - multi-tracer efficiency
   - 'resolve' near grid-scale features
   - consistency: mass-tracer, preserve relative concentrations
   - accuracy on 'fancy' spherical grids (test case)
   - geometric flexibility

2. Conservative Semi-LAgrangian Multi-tracer (CSLAM) scheme
   - scheme basics

3. Flux-form version of CSLAM (FF-CSLAM)
   - semi-Lagrangian flux-form method
   - experimentation with limiters/filters

4. New challenging test cases for transport schemes on the sphere

Why focus on transport schemes? Multi-tracer efficiency

Continuity equations in NCAR's Community Atmosphere Model (CAM) version 5

- Air density
- Water species: Water vapor, cloud liquid water and ice
- Microphysics & Aerosols: number concentrations (cloud water variables, aerosols), particulate organic matter, dust, sea salt, secondary organic aerosols, ... (**total of 22**)

Why focus on transport schemes?

Continuity equations in NCAR's Community Atmosphere Model (CAM) version 5

- Air density
- Water species: Water vapor, cloud liquid water and ice
- Microphysics & Aerosols: number concentrations (cloud water variables, aerosols), particulate organic matter, dust, sea salt, secondary organic aerosols, ... (**total of 22**)

Continuity equations in Chemistry version of CAM

Prognoses 126+ chemical species (computational cost of resolved scale transport is substantial also compared to parameterizations of sub-grid-scale chemical processes).

Why focus on transport schemes?

Continuity equations in NCAR's Community Atmosphere Model (CAM) version 5

- Air density
- Water species: Water vapor, cloud liquid water and ice
- Microphysics & Aerosols: number concentrations (cloud water variables, aerosols), particulate organic matter, dust, sea salt, secondary organic aerosols, ... (**total of 22**)

Continuity equations in Chemistry version of CAM

Prognoses 126+ chemical species (computational cost of resolved scale transport is substantial also compared to parameterizations of sub-grid-scale chemical processes).

$\hookrightarrow$ *In many atmospheric modeling applications the computational cost of resolved dynamics is (or is expected to be) dominated by the cost of tracer transport*

$\hookrightarrow$ *Multi-tracer efficiency is becoming increasingly important*

Example from CAM5 at $1.9^\circ \times 2.5^\circ$ resolution

Water variables

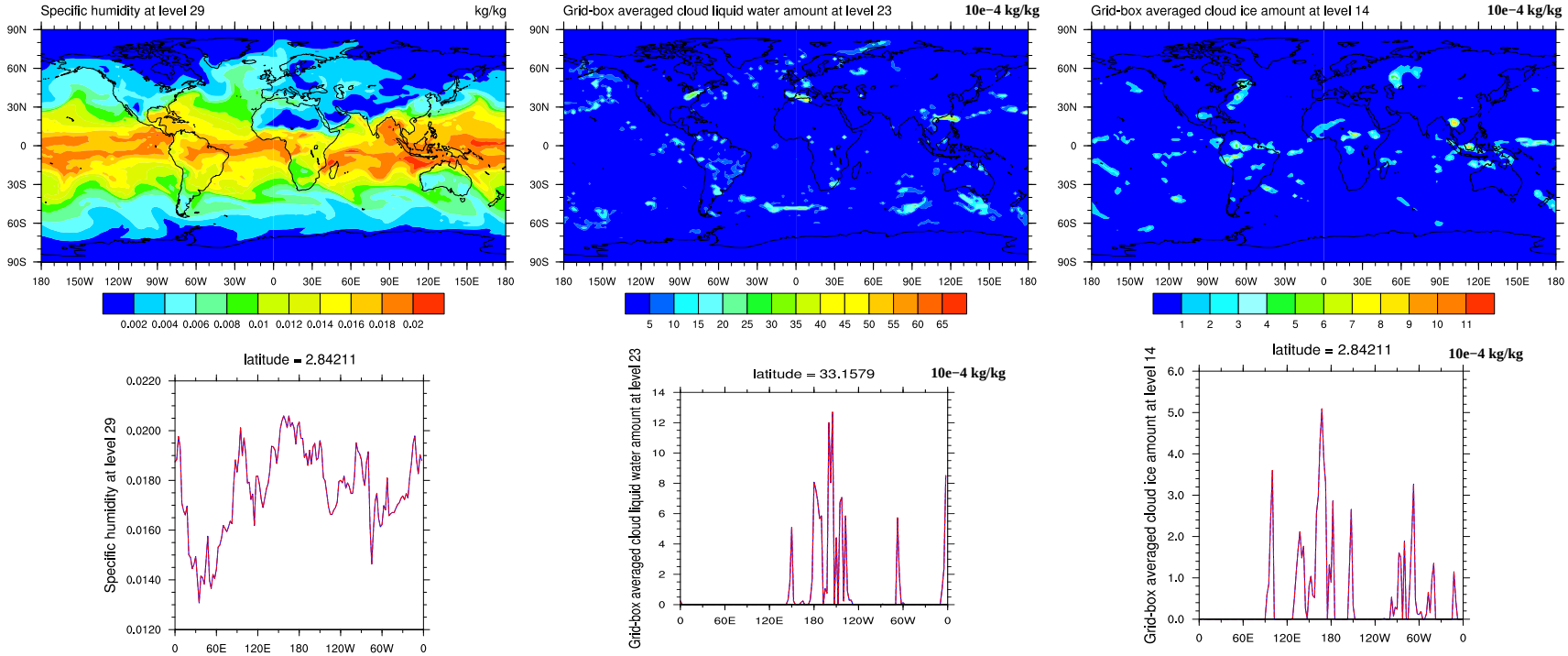

- many fields (water variables, aerosols, chemical species, ...) contain near grid-scale features
- production/loss terms are large, however, locally the advective tendency can be large (e.g., cloud ice mixing ratio for Cirrus, aerosols, ...)

Example from CAM5 at $1.9^\circ \times 2.5^\circ$ resolution

Aerosol number concentration

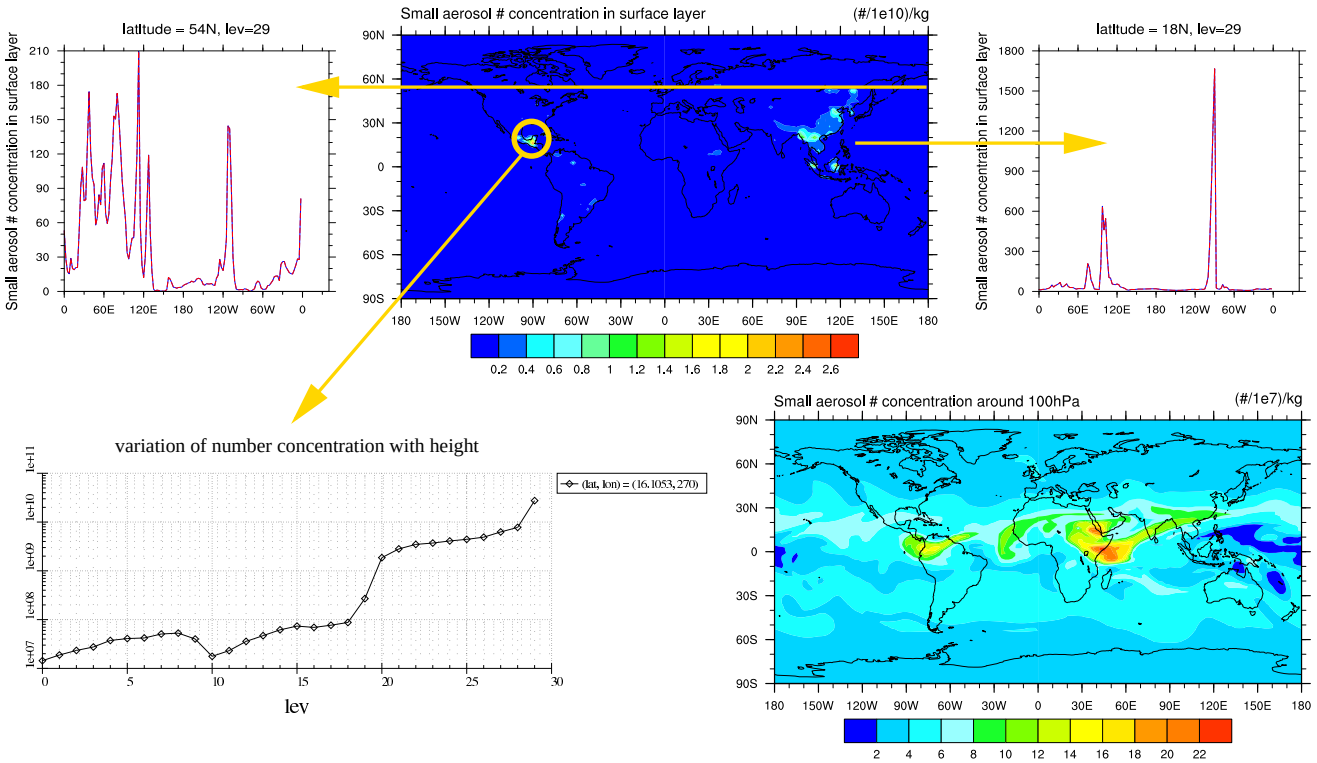

- many fields (water variables, aerosols, chemical species, ...) contain near grid-scale features
- production/loss terms are large, however, locally the advective tendency can be large (e.g., cloud ice mixing ratio for Cirrus, aerosols, ...)

Aerosols: Eruption under the Eyjafjallajökull glacier (left); Meteosat-9, April 15 (8AM) (right)

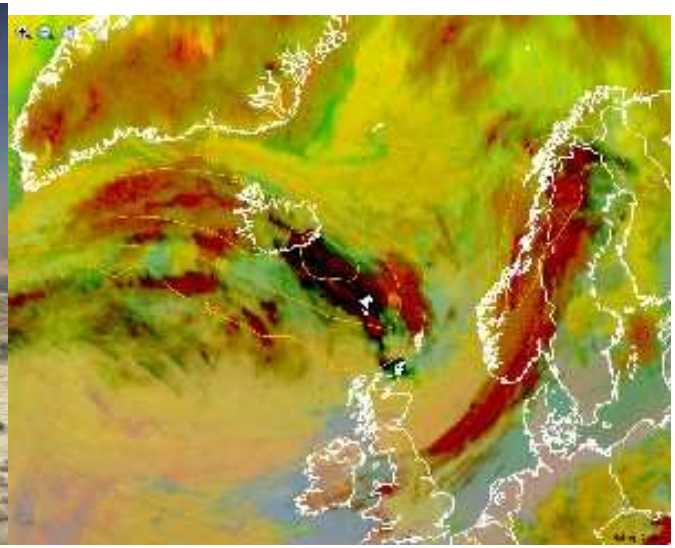

- many fields (water variables, aerosols, chemical species, ...) contain near grid-scale features
- production/loss terms are large, however, locally the advective tendency can be large (e.g., cloud ice mixing ratio for Cirrus, aerosols, ...)

Example from CAM5 at $1.9^\circ \times 2.5^\circ$ resolution

Br: Strong diurnal cycle (produced by photolysis)

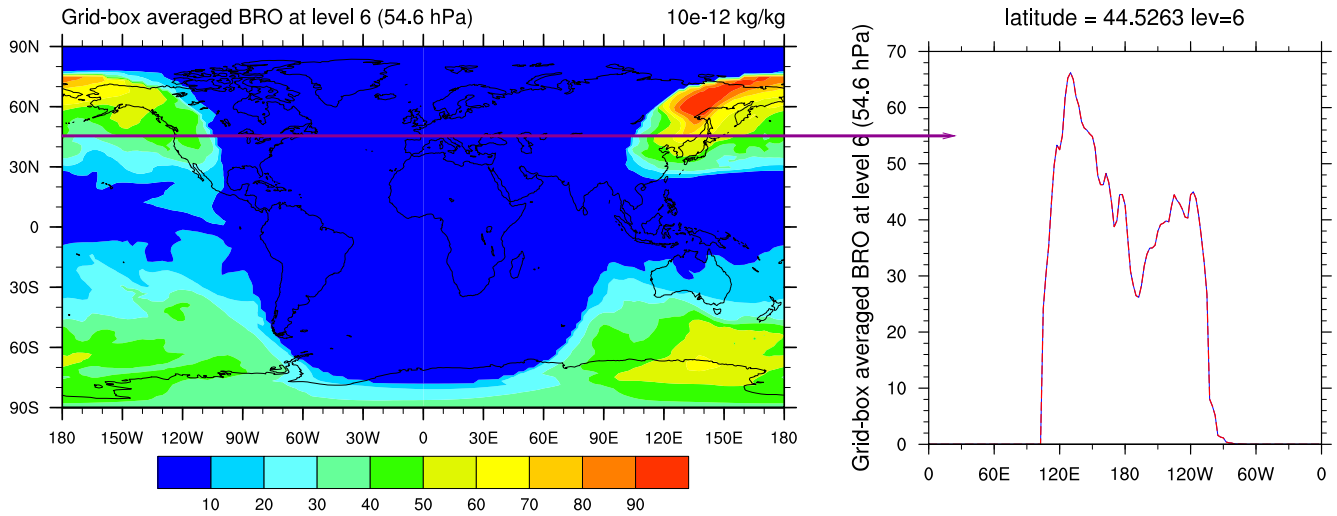

- many fields (water variables, aerosols, chemical species, ...) contain near grid-scale features
- production/loss terms are large, however, locally the advective tendency can be large (e.g., cloud ice mixing ratio for Cirrus, aerosols, ...)

Why focus on transport schemes? Consistency

- Air mass and tracer mass consistency:

$$\frac{\partial \rho}{\partial t} + \nabla \cdot (\rho \vec{v}) = 0, \tag{1}$$

$$\frac{\partial (\rho\, q)}{\partial t} + \nabla \cdot (\rho\, q \vec{v}) = 0, \tag{2}$$

  where $\vec{v}$ is the velocity vector, ρ is density for dry air $(\mathrm{kg/V})$ and q concentration (mixing ratio, $\mathrm{kg/kg}$). *If $q = 1$ then (2) reduces to (1).*

- Monotonicity: Note that (1) and (2) imply

$$\frac{dq}{dt} = 0, \quad \frac{d}{dt} \equiv \frac{\partial}{\partial t} + \vec{v} \cdot \nabla, \tag{3}$$

  q is conserved along trajectories/characteristics of the flow.

  $\hookrightarrow$ **Requirement for monotonicity applies to q not $(\rho\, q)$!**

- If the flow is non-divergent $\nabla \cdot \vec{v} = 0$ and if the transport operator preserves a constant for non-divergent flow fields then you no longer need to distinguish between ρ and ρq when testing for monotonicity preservation!

Why focus on transport schemes? Consistency (cont.)

- Chemistry: **Relative concentrations control chemical reactions** & transport schemes should preserve them (at least in areas with no or little mixing)
  this is stronger than preservation of linear correlations: $q_1 = c\, q_2 + d$

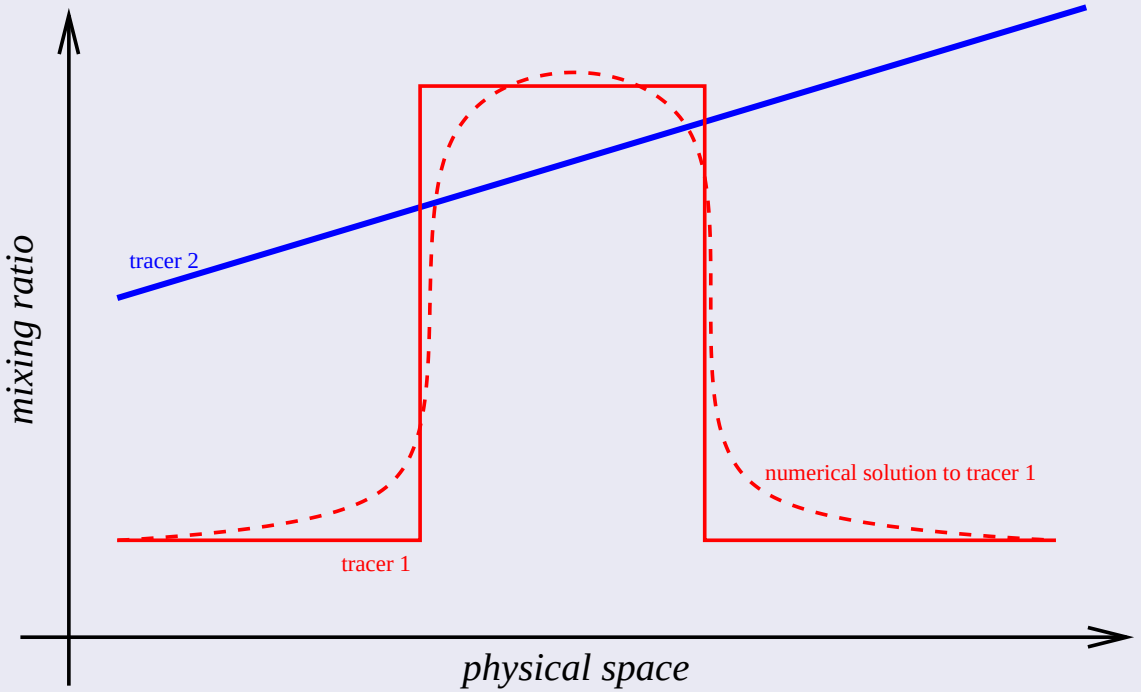

Figure: Assume constant wind. Most scheme can transport tracer 1 exactly but not tracer 2

Relative concentrations near large gradients are altered by numerical scheme ...

Why focus on transport schemes? 'Fancy' spherical grids

Primarily for scalability many groups are considering more isotropic spherical grids - challenges schemes in new ways:

- Grids are not orthogonal (at least not globally):
  - might question accuracy of dimensionally split schemes

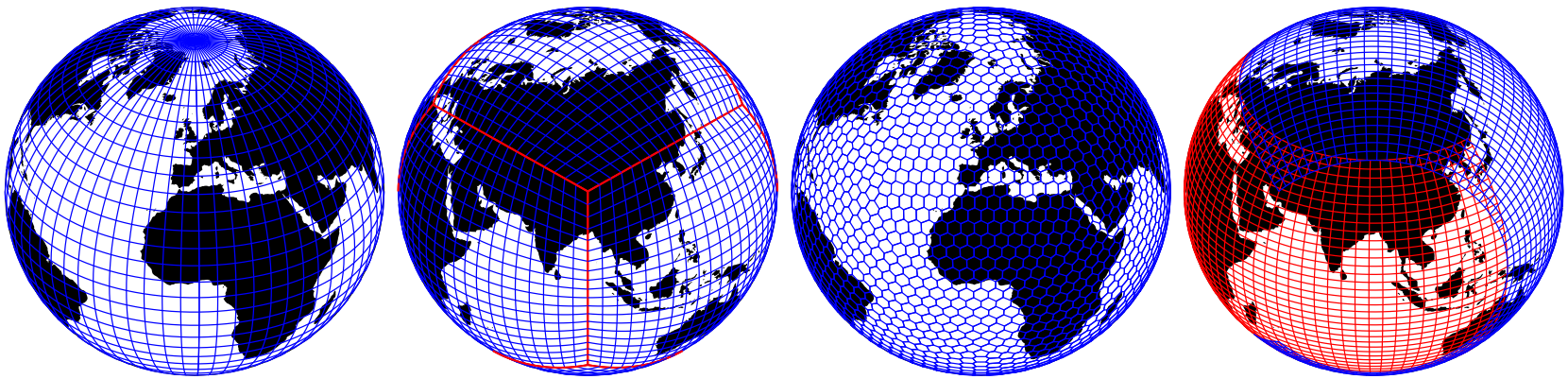

Why focus on transport schemes? 'Fancy' spherical grids

Primarily for scalability many groups are considering more isotropic spherical grids - challenges schemes in new ways:

- Grids are not orthogonal (at least not globally):
  - might question accuracy of dimensionally split schemes

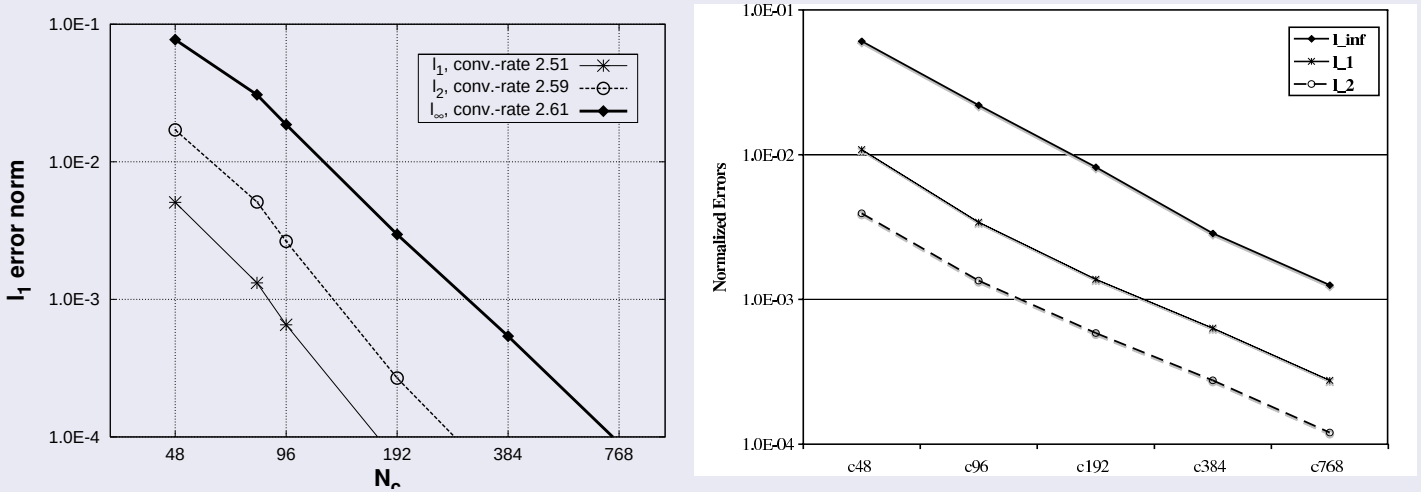

Convergence plots for moving vortices test case (Nair and Jablonowski, 2008): (left) CSLAM monotone, (right) Putman and Lin (2007)

- CSLAM and Putman and Lin (2007)-scheme use the same order of reconstruction function; main difference: fully 2D and dimensionally split, respectively!

Why focus on transport schemes? 'Fancy' spherical grids

Primarily for scalability many groups are considering more isotropic spherical grids - challenges schemes in new ways:

- Grids are not orthogonal (at least not globally):
  - might question accuracy of dimensionally split schemes
- Zonal flow is newer always aligned with grid lines as for the lat-lon grid

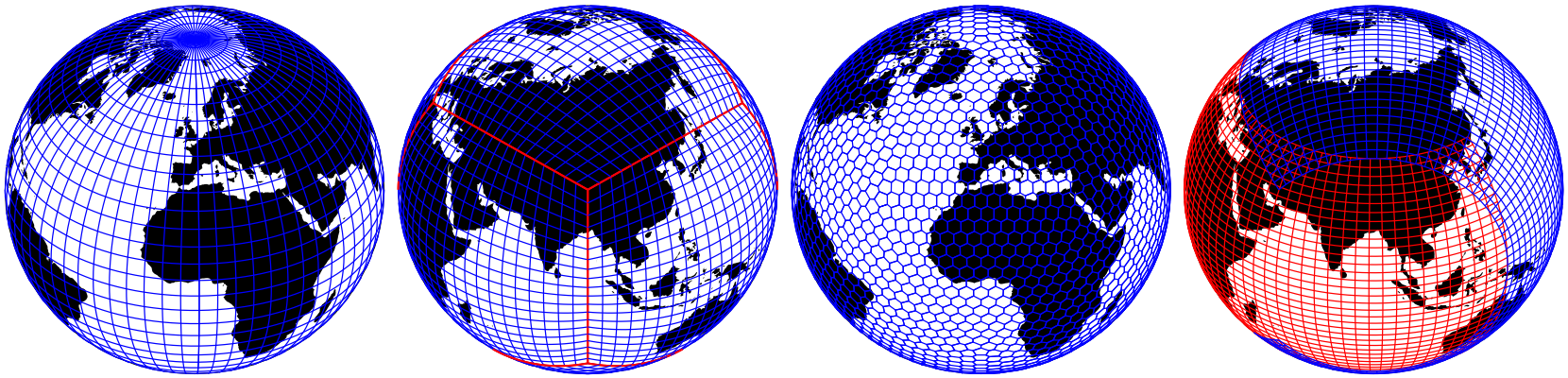

Rotated steady-state test case at 1° & 2° (Lauritzen, Jablonowski, Taylor and Nair, 2010a)

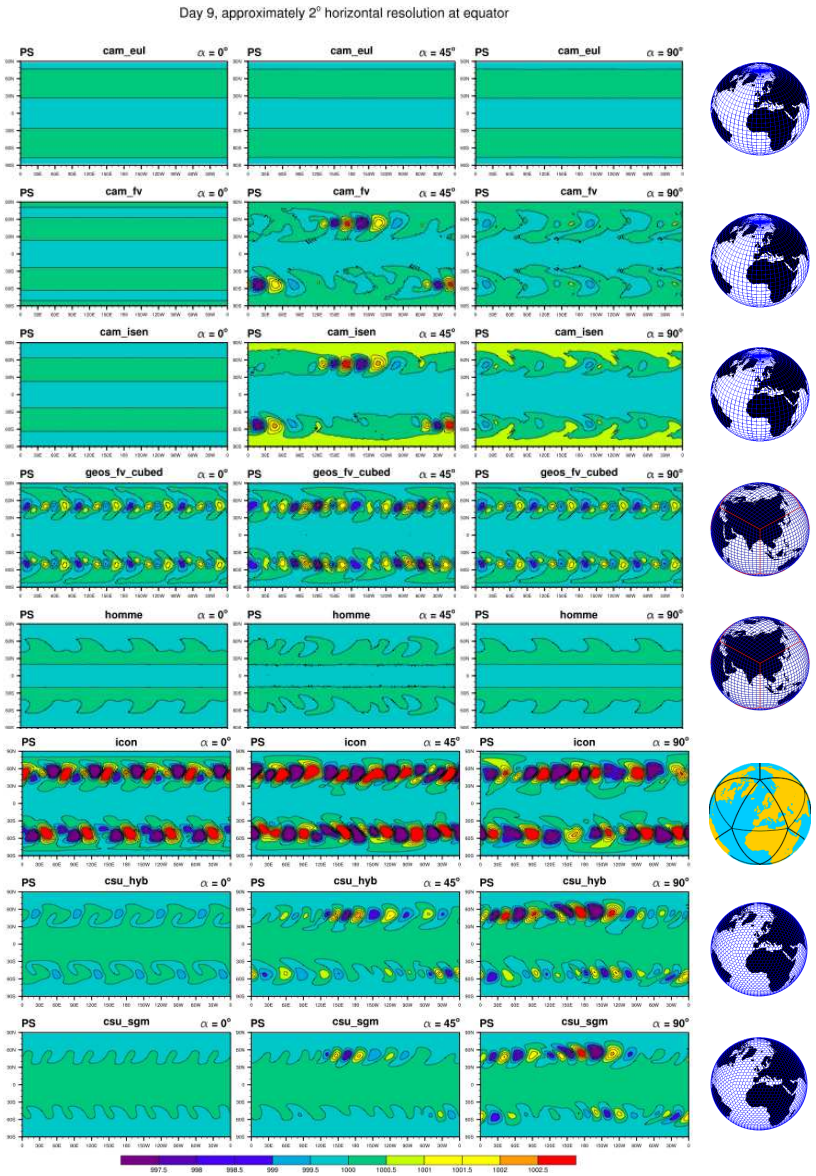

Rotate computational grid
(physical flow stays the same)

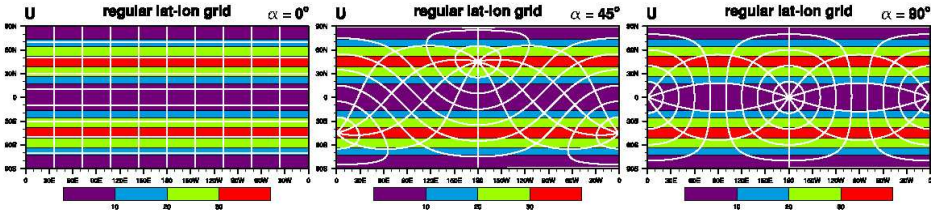

- Setup:
  - balanced steady state initial conditions (ps=1000 hPa for all t)
  - rotate computational grid (solutions should be invariant under rotation of computational grid)
- Baroclinically unstable flow (so any perturbation will grow.

Amplitude of spurious waves vary significantly among models (decreases with resolution)

- Definition: If $\ell_2 > 0.5$ then model is unable to maintain balanced flow

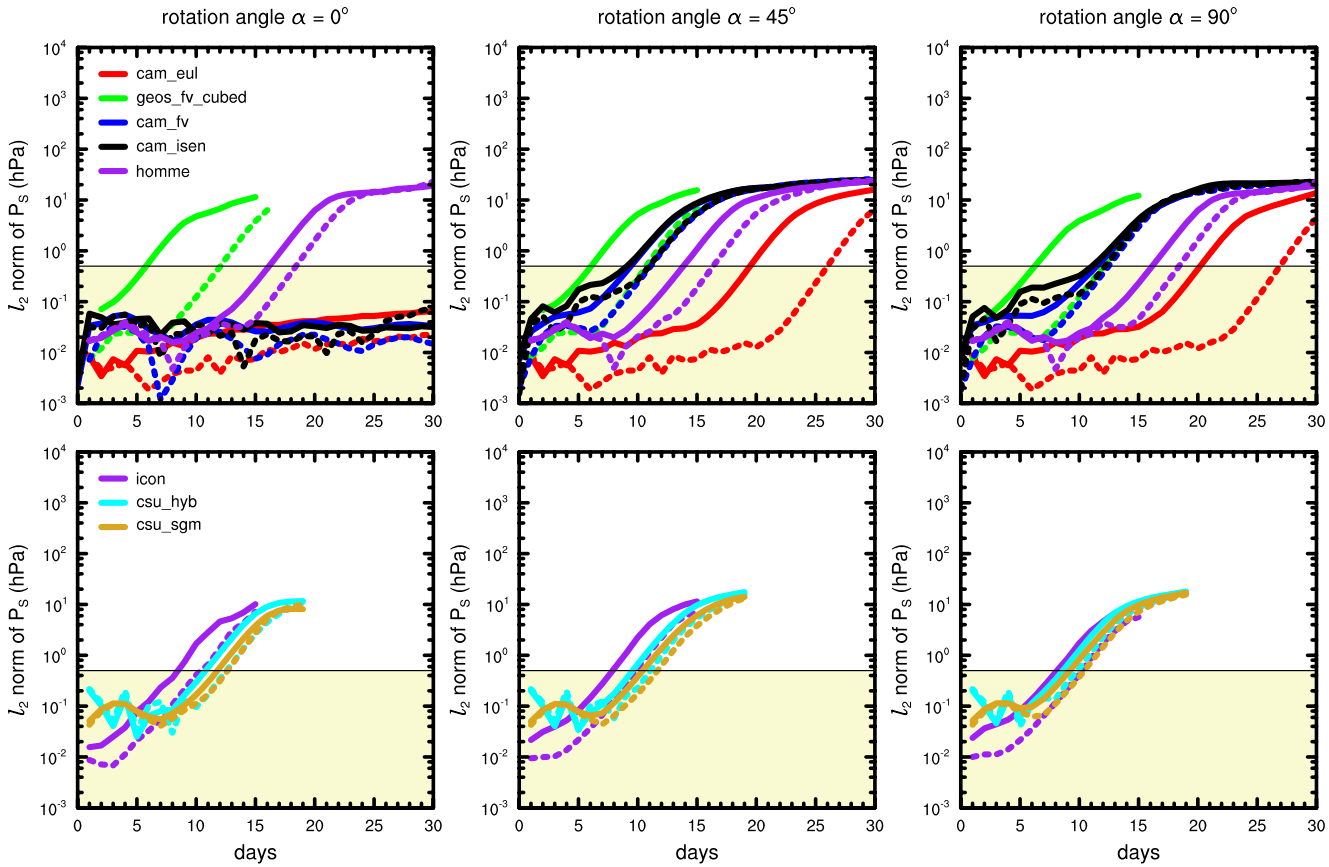

- Tendency for these models: Higher order and rigorous 2D treatment of grid 'non-uniformities' seems to lead to better solutions
- Open question: How many days should a model be able to maintain a balanced flow before it will spuriously impact long 'real' model simulations? (minimum resolution)

Commercial break

Lecture Notes in Computational Science and Engineering

- Springer book entitled 'Numerical Techniques for Global Atmospheric Models' based on the lectures given at the 2008 NCAR ASP (Advance Study Program) Summer Colloquium.
- Editors: P.H. Lauritzen, C. Jablonowski, M.A. Taylor and R.D. Nair
- 16 Chapters; authors include J.Thuburn, J.Tribbia, D.Durran, T.Ringler, W.Skamarock, R.Rood, J.Dennis, Editors, ...
- Publication date: Tentatively late 2010 or early 2011
- More details at: http://www.cgd.ucar.edu/cms/pel/colloquium.html and http://www.cgd.ucar.edu/cms/pel/lncse.html

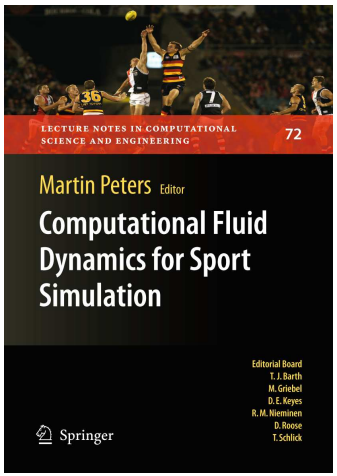

This book surveys recent developments in numerical techniques for global atmospheric models. It is based upon a collection of lectures prepared by leading experts in the field. The chapters reveal the multitude of steps that determine the global atmospheric model design. They encompass the choice of the equation set, computational grids on the sphere, horizontal and vertical discretizations, time integration methods, filtering and diffusion mechanisms, conservation properties, tracer transport, and considerations for designing models for massively parallel computers. A reader interested in applied numerical methods but also the many facets of atmospheric modeling should find this book of particular relevance.

End of commercial break

CSLAM & FF-CSLAM

So I hope I have convinced you that:

- multi-tracer efficiency is important
- consistency is important
- preservation of gradients (relative concentrations) is important
- geometric flexibility is important
- for 'fancy' grid models fully 2D advection schemes may significantly increase accuracy
- need to assess minimum resolution for models for which 'grid-imprinting' is not spuriously perturbing the solution (at least for models intended for long runs, e.g., paleo-climate applications, low frequency variability studies, ...)

Next:

- Geometrically flexible scheme: CSLAM and FF-CSLAM
- CSLAM was presented at PDEs on the sphere workshop in 2009 and has been published in J. Comp. Phys. (Lauritzen et al., 2010b)

$\rightarrow$ **only brief discussion here**

Conservative Semi-LAgrangian Multi-tracer (CSLAM)

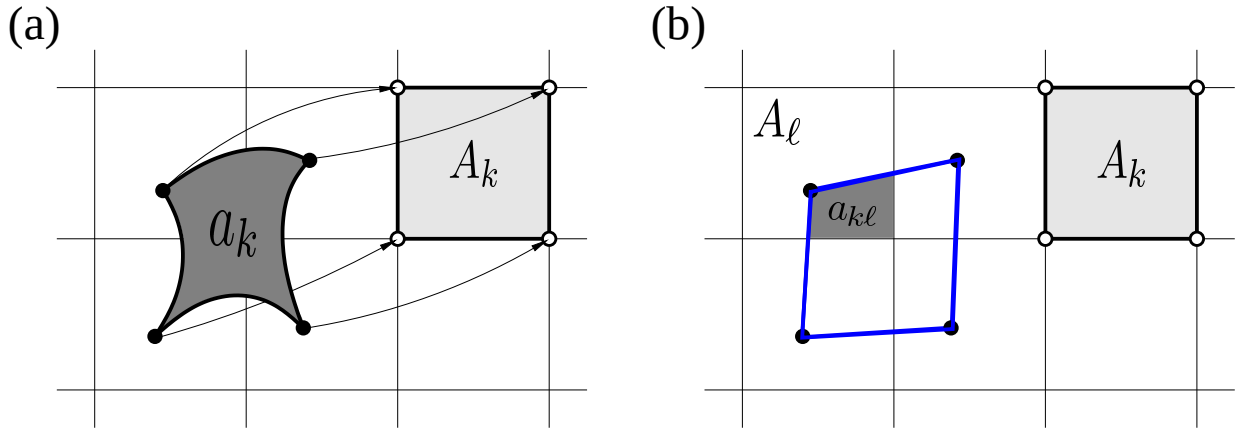

Finite-volume Lagrangian form of continuity equation for $\psi = \rho, \rho\, q$:

$$\int_{A_k} \psi_k^{n+1}\, dx\, dy = \int_{a_k} \psi_k^{n}\, dx\, dy \quad = \quad \sum_{\ell=1}^{L_k} \iint_{a_{k\ell}} f_\ell(x,y)\, dx\, dy,$$

where the $a_{k\ell}$'s are non-empty overlap regions:

$$a_{k\ell} = a_k \cap A_\ell, \quad a_{k\ell} \neq \emptyset; \quad \ell = 1, \ldots, L_k. \tag{1}$$

Conservative Semi-LAgrangian Multi-tracer (CSLAM)

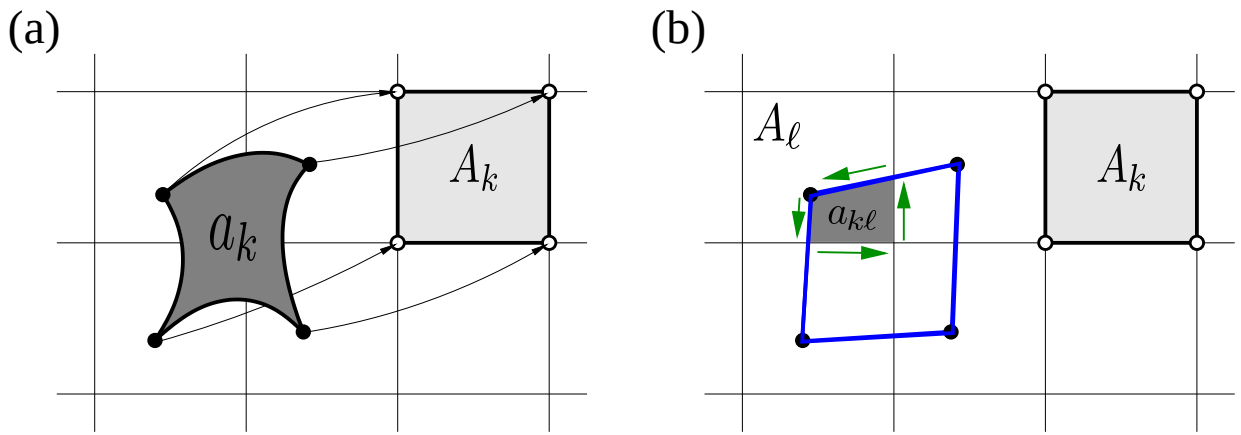

Finite-volume Lagrangian form of continuity equation for $\psi = \rho, \rho\, q$:

$$\int_{A_k} \psi_k^{n+1}\, dx\, dy = \int_{a_k} \psi_k^{n}\, dx\, dy \quad = \quad \sum_{\ell=1}^{L_k} \oint_{\partial a_{k\ell}} [P\, dx + Q\, dy]\,,$$

where $\partial a_{k\ell}$ is the boundary of $a_{k\ell}$ and

$$-\frac{\partial P}{\partial y} + \frac{\partial Q}{\partial x} = f_\ell(x, y) = \sum_{i+j \leqslant 2} c_\ell^{(i,j)} x^i y^j.$$

Conservative Semi-LAgrangian Multi-tracer (CSLAM)

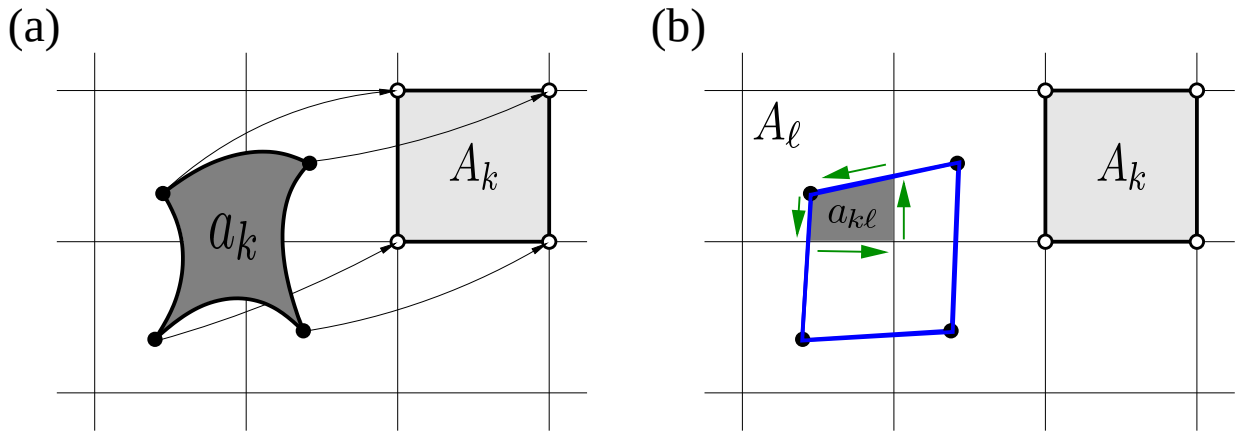

Finite-volume Lagrangian form of continuity equation for $\psi = \rho$, $\rho\, q$:

$$\int_{A_k} \psi_k^{n+1}\, dx\, dy = \int_{a_k} \psi_k^{n}\, dx\, dy \quad = \quad \sum_{\ell=1}^{L_k} \left[\sum_{i+j\leqslant 2} c_\ell^{(i,j)} w_{k\ell}^{(i,j)} \right],$$

where weights $w_{k\ell}^{(i,j)}$ are functions of the coordinates of the vertices of $a_{k\ell}$.

Conservative Semi-LAgrangian Multi-tracer (CSLAM)

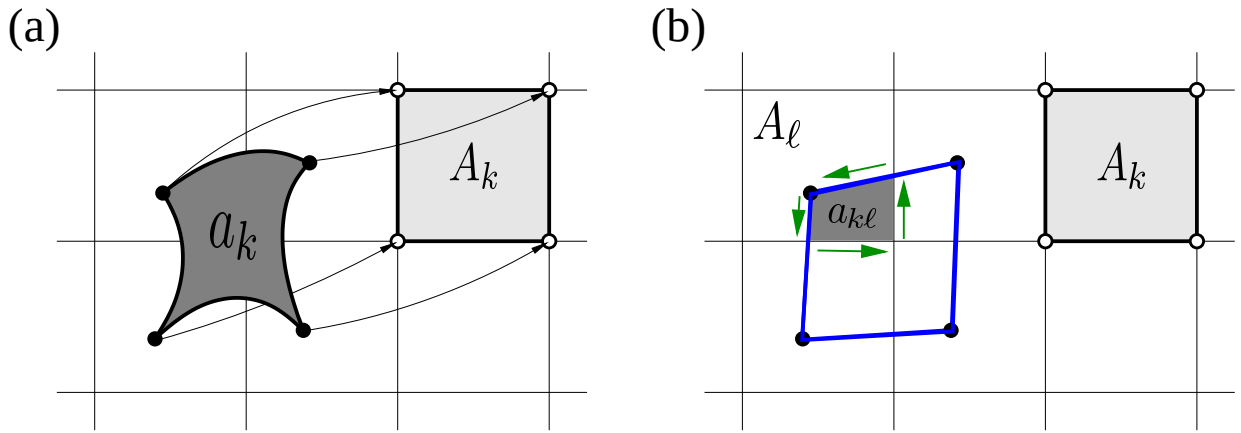

Finite-volume Lagrangian form of continuity equation for $\psi = \rho, \rho\, q$:

$$\int_{A_k} \psi_k^{n+1}\, dx\, dy = \int_{a_k} \psi_k^{n}\, dx\, dy \quad = \quad \sum_{\ell=1}^{L_k} \left[\sum_{i+j\leqslant 2} c_\ell^{(i,j)} w_{k\ell}^{(i,j)} \right],$$

- $w_{k\ell}^{(i,j)}$ can be re-used for each additional tracer (Dukowicz and Baumgardner, 2000)
- computational cost for each additional tracer is the reconstruction and limiting/filtering.
- CSLAM is stable for long time-steps (CFL>1)

- Equi-angular cubed-sphere extension of CSLAM discussed next ....
- CSLAM is fully two-dimensional and can be extended to any spherical grid constructed from great-circle arcs.

Gnomonic projection

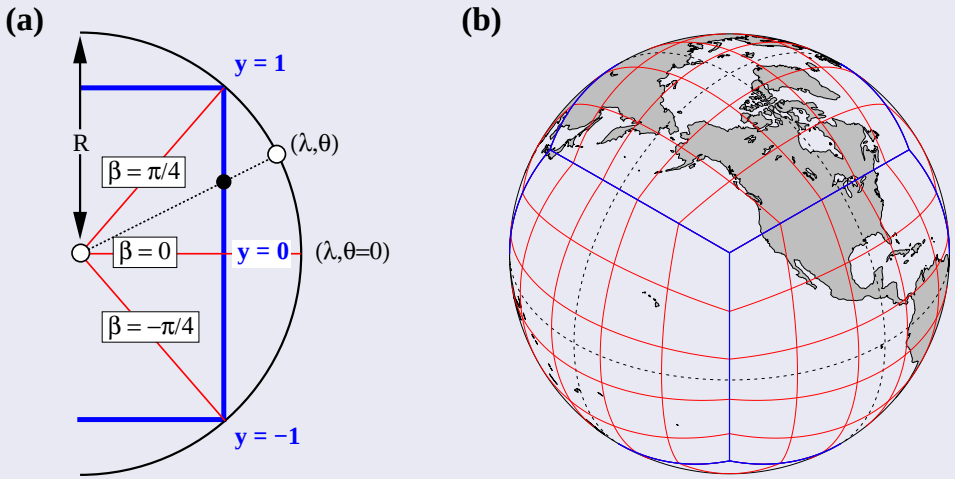

- Computational space is 'Cartesian-like' gnomonic coordinates (x, y) (Sadourny, 1972) defined in terms of central angles (α, β):

$$x = \tan\alpha \quad \text{and} \quad y = \tan\beta; \quad \alpha, \beta \in \left[-\frac{\pi}{4}, \frac{\pi}{4}\right], \tag{1}$$

- any straight line on the gnomonic projection corresponds to a great-circle arc
- $\Rightarrow$ reuse Cartesian algorithm except:
  - Divergence theorem must be converted to gnomonic coordinates (Ullrich, Lauritzen and Jablonowski, 2009).
  - Consistently couple the panel discretizations for the global domain.

Divergence theorem in gnomonic coordinates

Let Ψ be a vector field with contravariant components Ψ_x and Ψ_y in the direction of the unit basis vectors (e_x, e_y), i.e. $\Psi = \Psi_x e_x + \Psi_y e_y$. Divergence theorem:

$$\int_{A_{k\ell}} \nabla \cdot \Psi dV = -\oint_{\partial a_{k\ell}} \left[\widetilde{\Psi}_x \, dy + \widetilde{\Psi}_y \, dx \right], \tag{2}$$

where

$$\widetilde{\Psi}_x = \frac{\Psi_x}{\rho \sqrt{1+y^2}} \text{ and } \widetilde{\Psi}_y = \frac{\Psi_y}{\rho \sqrt{1+x^2}},$$

with $\rho = \sqrt{1+x^2+y^2}$. The divergence operator is given by

$$\nabla \cdot \Psi = \rho^3 \left[\frac{\partial \widetilde{\Psi}_x}{\partial x} + \frac{\partial \widetilde{\Psi}_y}{\partial y} \right]. \tag{3}$$

Divergence theorem in gnomonic coordinates

A choice of potentials for fully 2D (third-order, '2D PPM') reconstructions:

$$\widetilde{\Psi}_x^{(i,j)}(x,y) = 0, \quad i,j \in \{0,1,2\} \tag{4}$$

$$\widetilde{\Psi}_y^{(0,0)}(x,y) = \frac{1}{1+x^2}\frac{y}{\rho}, \tag{5}$$

$$\widetilde{\Psi}_y^{(1,0)}(x,y) = \frac{1}{1+x^2}\frac{xy}{\rho}, \tag{6}$$

$$\widetilde{\Psi}_y^{(0,1)}(x,y) = -\frac{1}{\rho}, \tag{7}$$

$$\widetilde{\Psi}_y^{(2,0)}(x,y) = \frac{1}{1+x^2}\frac{x^2 y}{\rho}, \tag{8}$$

$$\widetilde{\Psi}_y^{(0,2)}(x,y) = -\frac{y}{\rho} + \operatorname{arcsinh}\left(\frac{y}{\sqrt{1+x^2}}\right), \tag{9}$$

$$\widetilde{\Psi}_y^{(1,1)}(x,y) = -\frac{x}{\rho}, \tag{10}$$

Divergence theorem in gnomonic coordinates

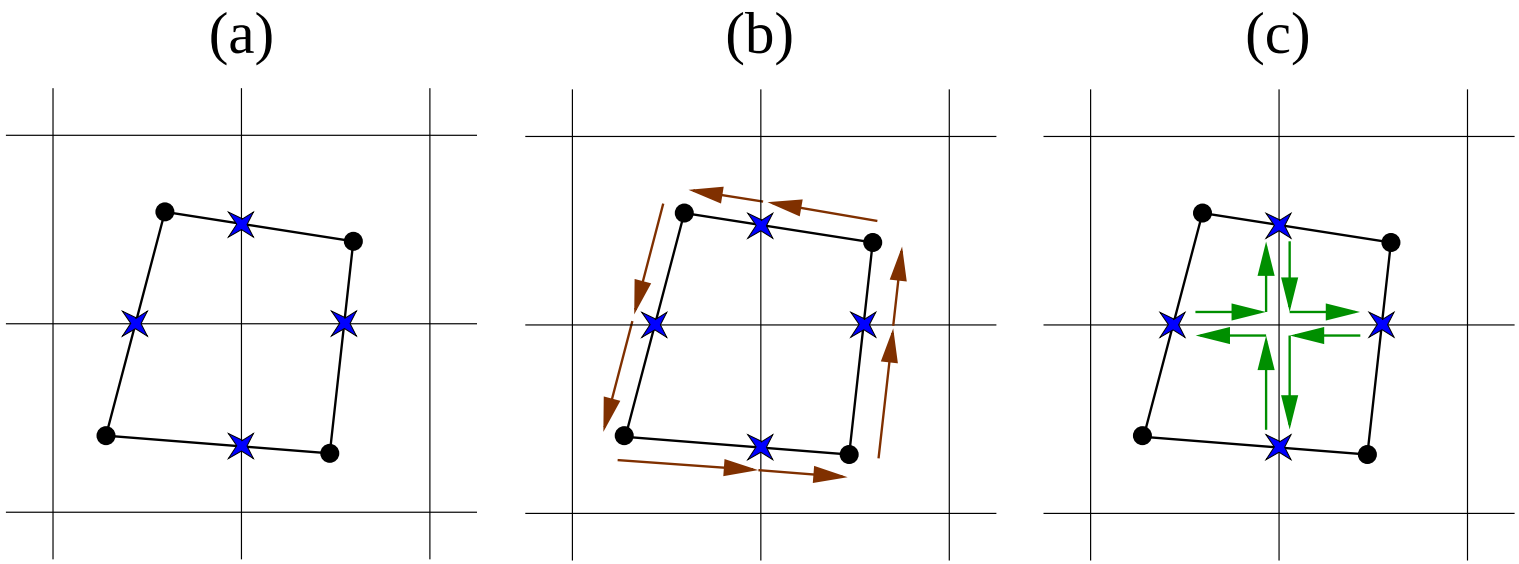

- Integrating the potentials along sides of $a_{k\ell}$:
  - (Fig. c) Along coordinates lines it is possible to compute the line integrals exactly (Ullrich, Lauritzen and Jablonowski, 2009).
  - (Fig. b) Along lines of arbitrary orientation we use 2-point Gaussian quadrature.

Coupling panels

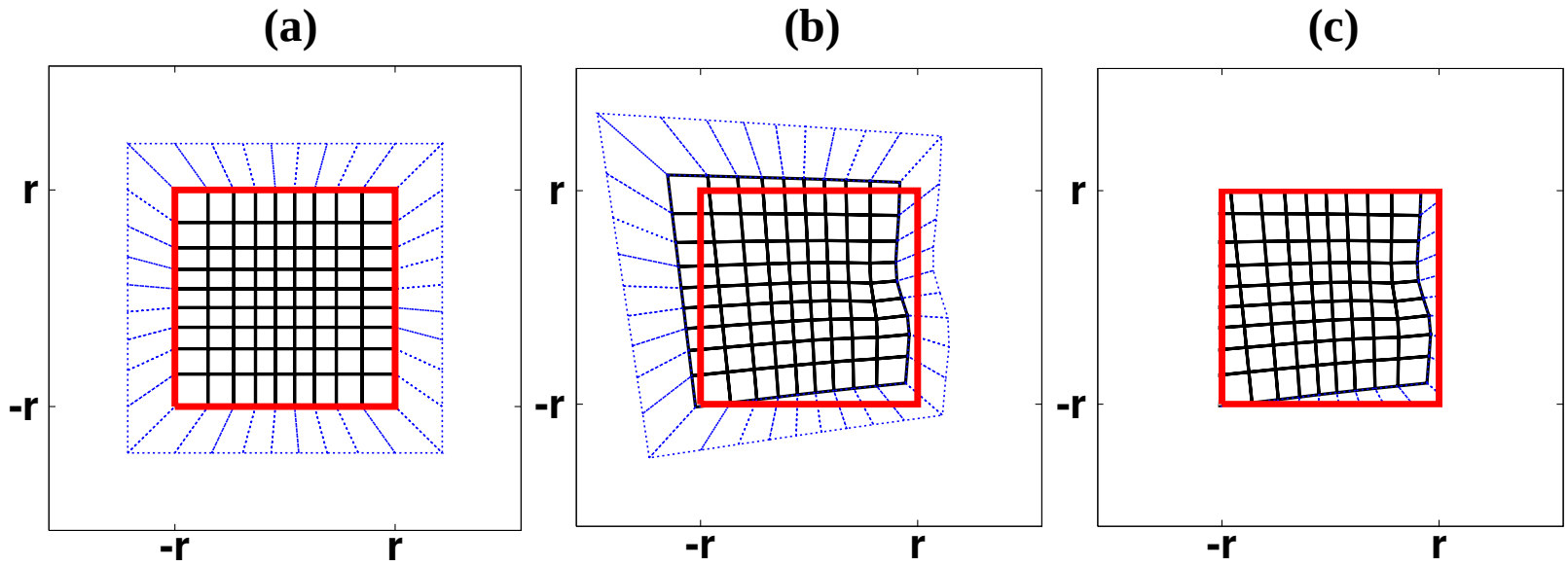

- (a) Halo for panel p (on panel p's projection). Note that the cells on neighboring panels are deformed on panel p's projection.
- (b) Compute deformed upstream grid (Figure shows upstream grid for moving vortex test case). Note that cells entering from neighboring panels are 'naturally' skewed
- (c) 'Chop off' non-local overlap areas
- Do remapping local to panel (for each panel)
- Collect contributions from neighboring panels.

Flux-form CSLAM (FF-CSLAM)

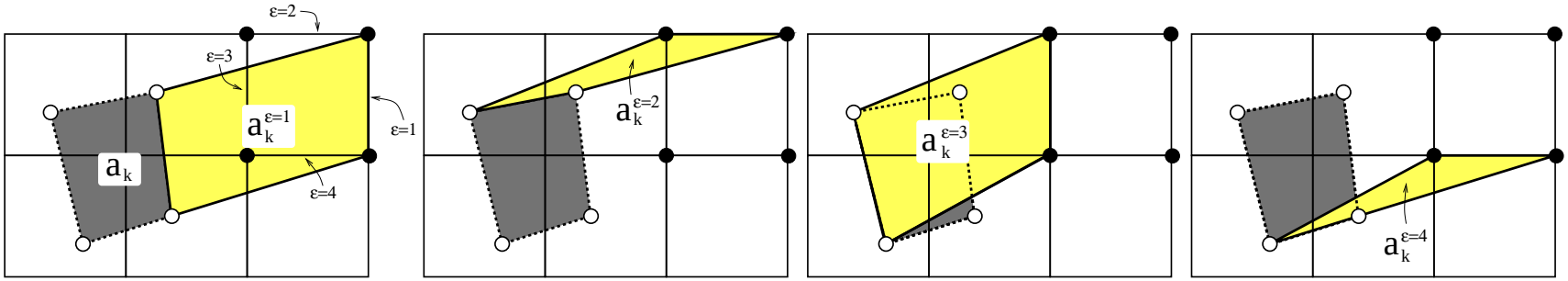

Finite-volume flux-form of continuity equation for $\psi = \rho, \rho\, q$:

$$\int_{A_k} \psi_k^{n+1}\, dx\, dy \quad = \quad \int_{A_k} \psi_k^{n}\, dx\, dy - \sum_{\epsilon=1}^{4} \left[\sum_{\ell=1}^{L_k^\epsilon} s_{k\ell}^\epsilon \iint_{a_{k\ell}^\epsilon} f_\ell(x,y)\, dx\, dy \right], \qquad (11)$$

where

- a_k^ϵ = 'flux-area' (yellow area) = area swept through face ϵ
- L_k^ϵ = number of overlap areas for a_k^ϵ; $a_{k\ell}^\epsilon = a_k^\epsilon \cap A_k$
- $s_{k\ell}^\epsilon = 1$ for outflow and -1 for inflow.
- **All technology developed for CSLAM can be re-used**

Flux-form CSLAM (FF-CSLAM)

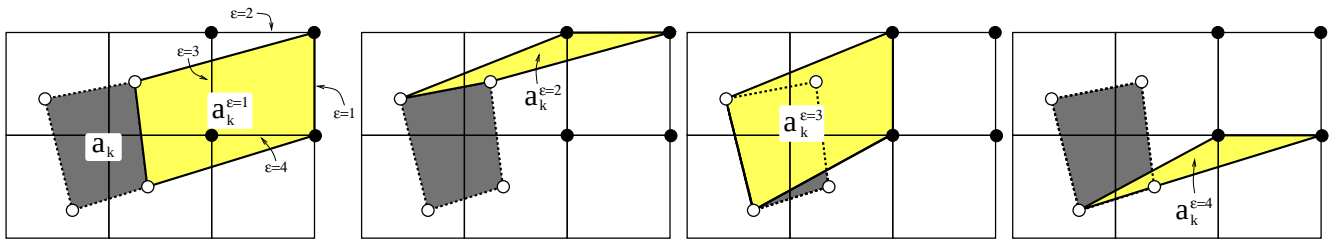

Finite-volume flux-form of continuity equation for $\psi = \rho, \rho\, q$:

$$\int_{A_k} \psi_k^{n+1}\, dx\, dy \quad = \quad \int_{A_k} \psi_k^{n}\, dx\, dy - \sum_{\epsilon=1}^{4} \left[\sum_{\ell=1}^{L_k^\epsilon} s_{k\ell}^\epsilon \iint_{a_{k\ell}^\epsilon} f_\ell(x,y)\, dx\, dy \right], \qquad (11)$$

- Note: all the areas involved in forecast (11) 'sum-up to' upstream Lagrangian area δa_k:

$$\Delta A_k - \sum_{\epsilon=1}^{4} \left[\sum_{\ell=1}^{L_k^\epsilon} s_{k\ell}^\epsilon \delta a_k^\epsilon \right] = \delta a_k. \qquad (12)$$

  Aside: in flux-form you'll conserve mass even when you are 'sloppy' about approximating a_k^ϵ, that is, effective upstream areas δa_k do not need to span the domain without overlaps/gaps as for the Lagrangian scheme! (**However, for consistency and maybe accuracy it should be the case** - **geometric error**)

- One tracer: For $\mathrm{CFL} < 1$ FF-CSLAM is at most 40% more expensive than CSLAM (for CFL$\approx$3 FF-CSLAM is approximately 110% more expensive than CSLAM)

$\rightarrow$ Why FF-CSLAM?

Flux-form CSLAM (FF-CSLAM)

- In CSLAM **shape-preservation** is enforced by filtering the sub-grid-cell reconstructions (also applicable for FF-CSLAM)
- Casting in flux-form one may also apply **flux-limiters** such as FCT (Flux-Correct-Transport, Zalesak 1979).
- Flux-form allows for **super-cycling (also referred to as sub-cycling)**, that is, transport tracers with longer time-steps than what is used for the dynamics.

$$(\rho\, q)^{n+1} = (\rho\, q)^{n} + \langle q^{n} \rangle \times \left[\sum_{i=1}^{ksplit} \delta\rho^{n+i/ksplit} \right], \tag{11}$$

where $\delta\rho^{n+i/ksplit}$ is the flux of air mass into the cell during one sub-cycled time-step $\Delta t/ksplit$, $ksplit$ is the number of 'dynamics' time-steps per tracer time-step, $\langle q^{n} \rangle$ is the average of q over brown area:

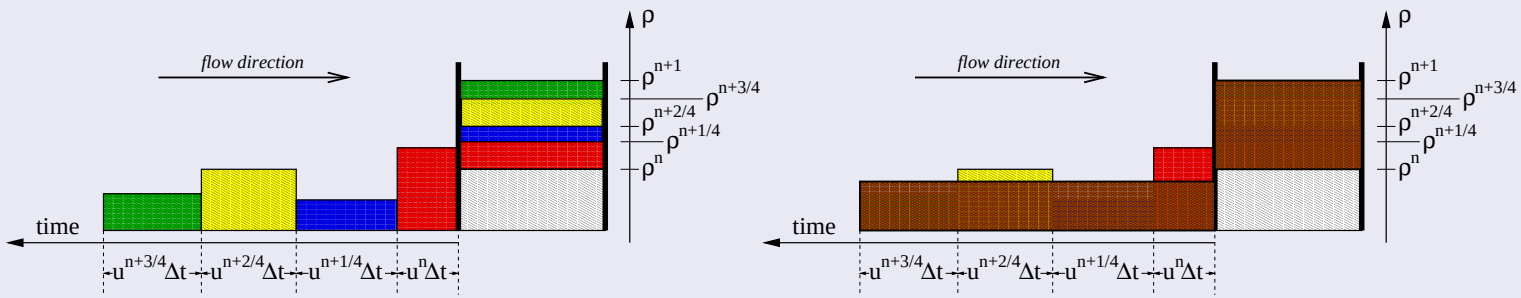

Figure: Assume no flow through right cell boundary

Flux-form CSLAM (FF-CSLAM)

- In CSLAM **shape-preservation** is enforced by filtering the sub-grid-cell reconstructions (also applicable for FF-CSLAM)
- Casting in flux-form one may also apply **flux-limiters** such as FCT (Flux-Correct-Transport, Zalesak 1979).
- Flux-form allows for **super-cycling (also referred to as sub-cycling)**, that is, transport tracers with longer time-steps than what is used for the dynamics.

$$(\rho\, q)^{n+1} = (\rho\, q)^{n} + \langle q^{n} \rangle \times \left[\sum_{i=1}^{ksplit} \delta\rho^{n+i/ksplit} \right], \tag{11}$$

Note that if $q = 1$ then the equation reduces to the discrete continuity equation for air (air-tracer mass consistency)

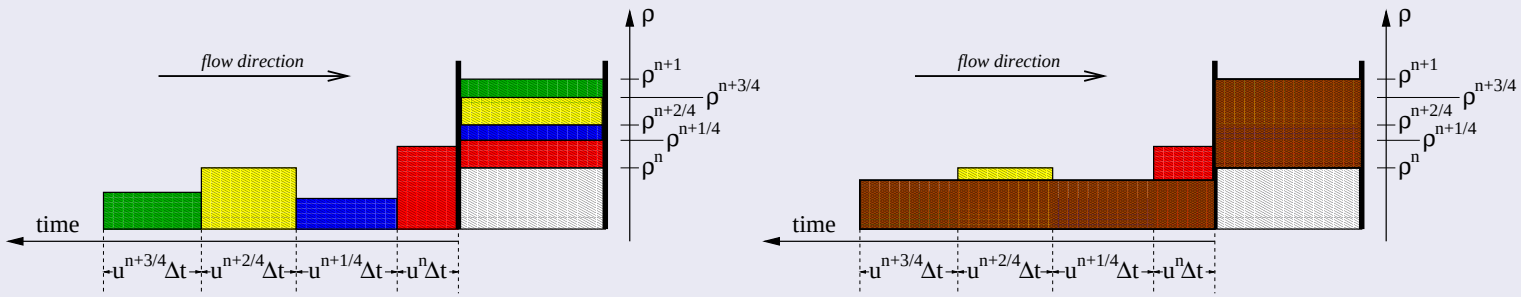

Figure: Assume no flow through right cell boundary

Limiters and filters

- **In the literature: Many 1D limiters but few fully 2D limiters!**
- A priori ('**Monotone filtering**'): Filter the reconstruction $f_\ell(x, y)$ so that extreme values lie within the adjacent cell-average values (Barth and Jespersen, 1989).

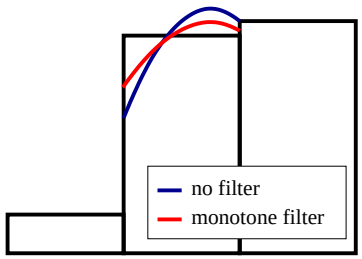

- A posteriori ('**Monotone limiting**'): Limit the fluxes to prevent new extrema in $\overline{\psi}^{n+1}$ using flux-corrected transport (Zalesak, 1979).

- Monotone filters/limiters tend to 'clip' physical extrema

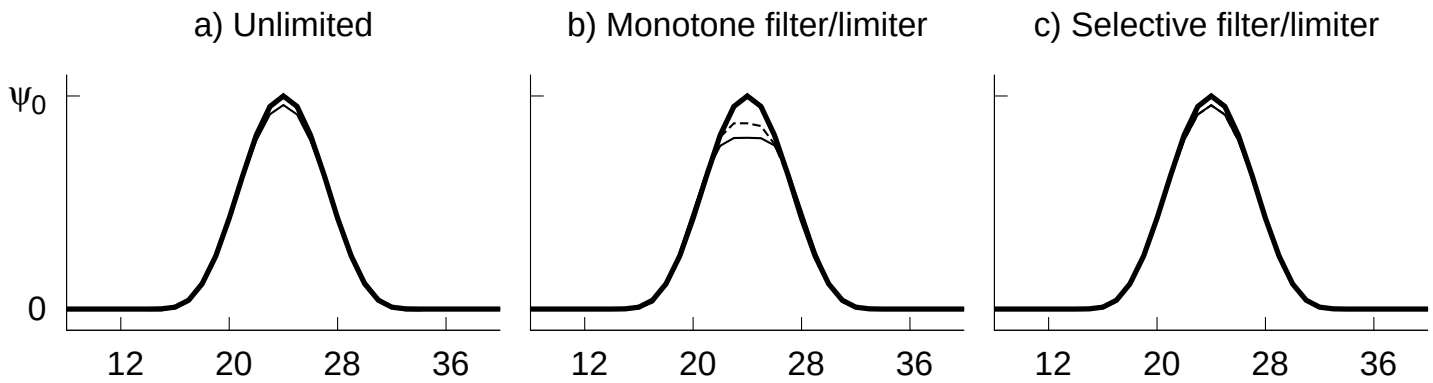

Limiters and filters

- **In the literature: Many 1D limiters but few fully 2D limiters!**
- A priori ('**Monotone filtering**'): Filter the reconstruction $f_\ell(x, y)$ so that extreme values lie within the adjacent cell-average values (Barth and Jespersen, 1989).

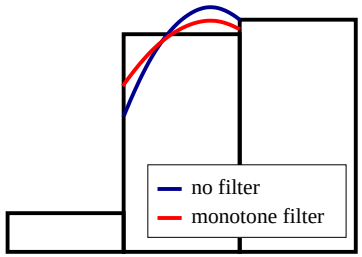

- A posteriori ('**Monotone limiting**'): Limit the fluxes to prevent new extrema in $\overline{\psi}^{n+1}$ using flux-corrected transport (Zalesak, 1979).

- **Selective filtering/selective limiting** (Blossey and Durran, 2008): apply filtering or limiting only where a WENO-based smoothness metric exceeds a certain threshold:

$$\gamma = \frac{1}{2}\left[\left(2\Delta x \frac{\partial f}{\partial x}\right)^2 + \left(\Delta x^2 \frac{\partial^2 f}{\partial x^2}\right)^2 + \left(2\Delta y \frac{\partial f}{\partial y}\right)^2 + \left(\Delta y^2 \frac{\partial^2 f}{\partial y^2}\right)^2 + \left(\Delta x \Delta y \frac{\partial^2 f}{\partial x \partial y}\right)^2\right] \tag{12}$$

Will render solution non-oscillatory but not strictly monotone ('miniscule' under- and over-shoots)

Limiters and filters

- **In the literature: Many 1D limiters but few fully 2D limiters!**
- A priori ('**Monotone filtering**'): Filter the reconstruction $f_\ell(x, y)$ so that extreme values lie within the adjacent cell-average values (Barth and Jespersen, 1989).

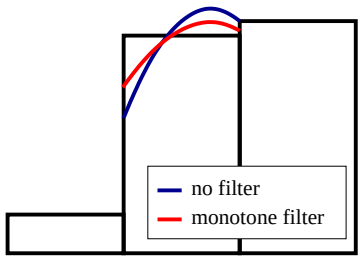

- A posteriori ('**Monotone limiting**'): Limit the fluxes to prevent new extrema in $\overline{\psi}^{n+1}$ using flux-corrected transport (Zalesak, 1979).

- Monotone filters/limiters tend to 'clip' physical extrema

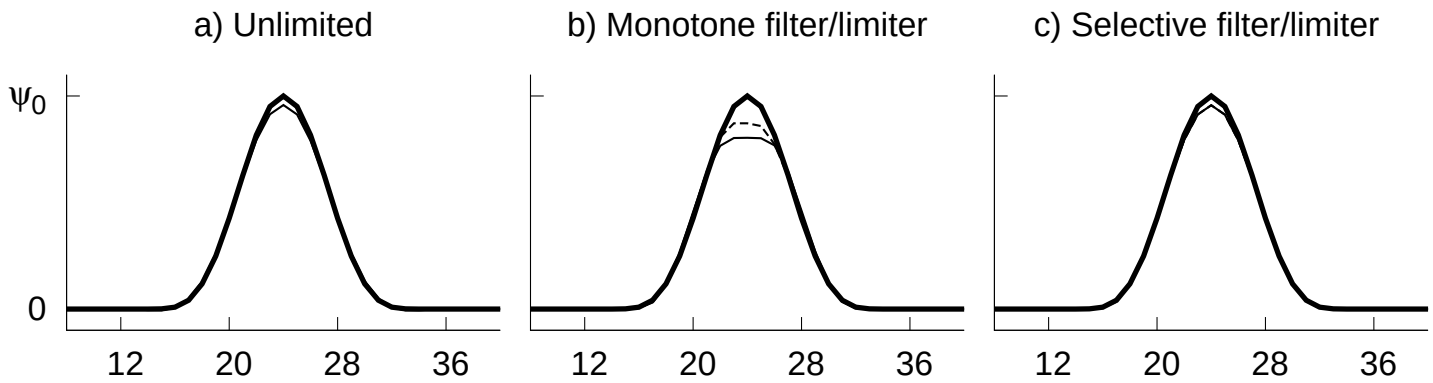

Flux-form CSLAM (FF-CSLAM): Results

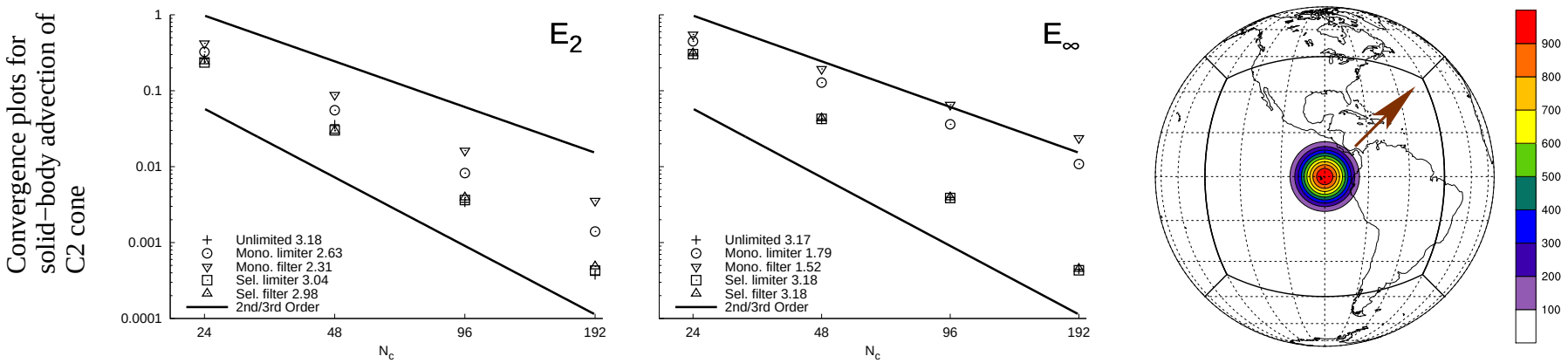

- Third-order convergence in E_2 and E_∞ for unlimited scheme and when using selective limiter/filter
- The monotone filtering is much less efficient than monotone limiting in FF-CSLAM (monotone limiting almost doubles the cost whereas monotone filtering almost triples the cost)
  $\rightarrow$ Computational cost of limiting is substantial (most likely also the case for other schemes?)!
- We also ran moving vortices test case (Nair and Jablonowski, 2008) as mentioned on earlier slide (Harris and Lauritzen 2010, submitted)

Idealized test cases for transport

Idealized test cases for transport

- Most transport schemes that have been implemented in global climate models have 'only' been tested (in idealized setup) for solid-body advection
  - No flow features of much interest (no deformation, no divergence, etc.):
  - Does not challenge schemes much
  - Preservation of a constant is easier compared to more complex non-divergent flows (Lagrangian areas undergo no deformation, rotation, etc.)
  - Does not force modelers to distinguish between tracer concentration q and tracer density $\rho\, q$

Idealized test cases for transport

- Most transport schemes that have been implemented in global climate models have 'only' been tested (in idealized setup) for solid-body advection
  - No flow features of much interest (no deformation, no divergence, etc.):
  - Does not challenge schemes much
  - Preservation of a constant is easier compared to more complex non-divergent flows (Lagrangian areas undergo no deformation, rotation, etc.)
  - Does not force modelers to distinguish between tracer concentration q and tracer density $\rho\, q$

- Need more rigorous benchmark test cases in a challenging environment to:
  - test schemes under divergent and deformational flow conditions
  - test schemes on new unstructured spherical grids
  - test static and dynamic mesh refinement algorithms
  - test trajectory algorithms (semi-Lagrangian or Lagrangian methods)

Idealized test cases for transport

- Most transport schemes that have been implemented in global climate models have 'only' been tested (in idealized setup) for solid-body advection
  - No flow features of much interest (no deformation, no divergence, etc.):
  - Does not challenge schemes much
  - Preservation of a constant is easier compared to more complex non-divergent flows (Lagrangian areas undergo no deformation, rotation, etc.)
  - Does not force modelers to distinguish between tracer concentration q and tracer density $\rho\, q$

- Need more rigorous benchmark test cases in a challenging environment to:
  - test schemes under divergent and deformational flow conditions
  - test schemes on new unstructured spherical grids
  - test static and dynamic mesh refinement algorithms
  - test trajectory algorithms (semi-Lagrangian or Lagrangian methods)

- **test case has to be simple to implement otherwise (most) people will not use it!**

Class of deformational test cases (Nair and Lauritzen 2010, in review)

- Very hard to derive complex flows that have an analytical solution for transport (for all t)
- So we follow ideas developed by LeVeque (1996) and use a time-reversing flow field, i.e. the exact solution after (t=T) = initial condition (t=0)

- Two non-divergent flow fields (k is flow parameter):
  - Case-1:

$$u(\lambda,\theta,t) = k\sin^2(\lambda/2)\sin(2\theta)\cos(\pi t/T) \quad (12)$$

$$v(\lambda,\theta,t) = \frac{k}{2}\sin(\lambda)\cos(\theta)\cos(\pi t/T) \quad (13)$$

$$\psi(\lambda,\theta,t) = k\sin^2(\lambda/2)\cos^2(\theta)\cos(\pi t/T). \quad (14)$$

    where ψ is the stream function: $u = -\frac{\partial\psi}{\partial\theta}, v = \frac{1}{\cos\theta}\frac{\partial\psi}{\partial\lambda}$
  - Case-2:

$$u(\lambda,\theta,t) = k\sin^2(\lambda)\sin(2\theta)\cos(\pi t/T) \quad (15)$$

$$v(\lambda,\theta,t) = k\sin(2\lambda)\cos(\theta)\cos(\pi t/T) \quad (16)$$

$$\psi(\lambda,\theta,t) = k\sin^2(\lambda)\cos^2(\theta)\cos(\pi t/T), \quad (17)$$

Class of deformational test cases (Nair and Lauritzen 2010, in review)

- Very hard to derive complex flows that have an analytical solution for transport (for all t)
- So we follow ideas developed by LeVeque (1996) and use a time-reversing flow field, i.e. the exact solution after (t=T) = initial condition (t=0)

- Two divergent flow fields (k is flow parameter):
  - Case-3:

$$u(\lambda,\theta,t) = -k\sin^2(\lambda/2)\sin(2\theta)\cos(\pi t/T) \quad (12)$$

$$v(\lambda,\theta,t) = \frac{k}{2}\sin(\lambda)\cos(\theta)\cos(\pi t/T) \quad (13)$$

  - Case-4:

$$u(\lambda,\theta,t) = -k\sin^2(\lambda/2)\sin(2\theta)\cos(\pi t/T) \quad (14)$$

$$v(\lambda,\theta,t) = -k\sin(\lambda)\cos^2(\theta)\cos(\pi t/T) \quad (15)$$

Class of deformational test cases (Nair and Lauritzen 2010, in review)

- For (semi-)Lagrangian schemes the trajectories can be computed using high-order Taylor Series expansions:

  The wind vector $\mathbf{V} = \mathrm{d}\mathbf{x}(\mathrm{t})/\mathrm{dt}$, and the upstream position of $\mathbf{x}_\mathrm{d}$ at the departure time $\mathrm{t} - \Delta\mathrm{t}$ is given by,

$$\mathbf{x}_\mathrm{d} \equiv \mathbf{x}(\mathrm{t} - \Delta\mathrm{t}) = \mathbf{x}(\mathrm{t}) - \Delta\mathrm{t}\,\frac{\mathrm{d}}{\mathrm{dt}}\mathbf{x}(\mathrm{t}) + \frac{(\Delta\mathrm{t})^2}{2!}\frac{\mathrm{d}^2}{\mathrm{dt}^2}\mathbf{x}(\mathrm{t}) - \cdots \tag{12}$$

$$\frac{\mathrm{d}\lambda}{\mathrm{dt}} = \frac{u}{\cos(\theta)} \qquad \frac{\mathrm{d}\theta}{\mathrm{dt}} = v$$

Class of deformational test cases (Nair and Lauritzen 2010, in review)

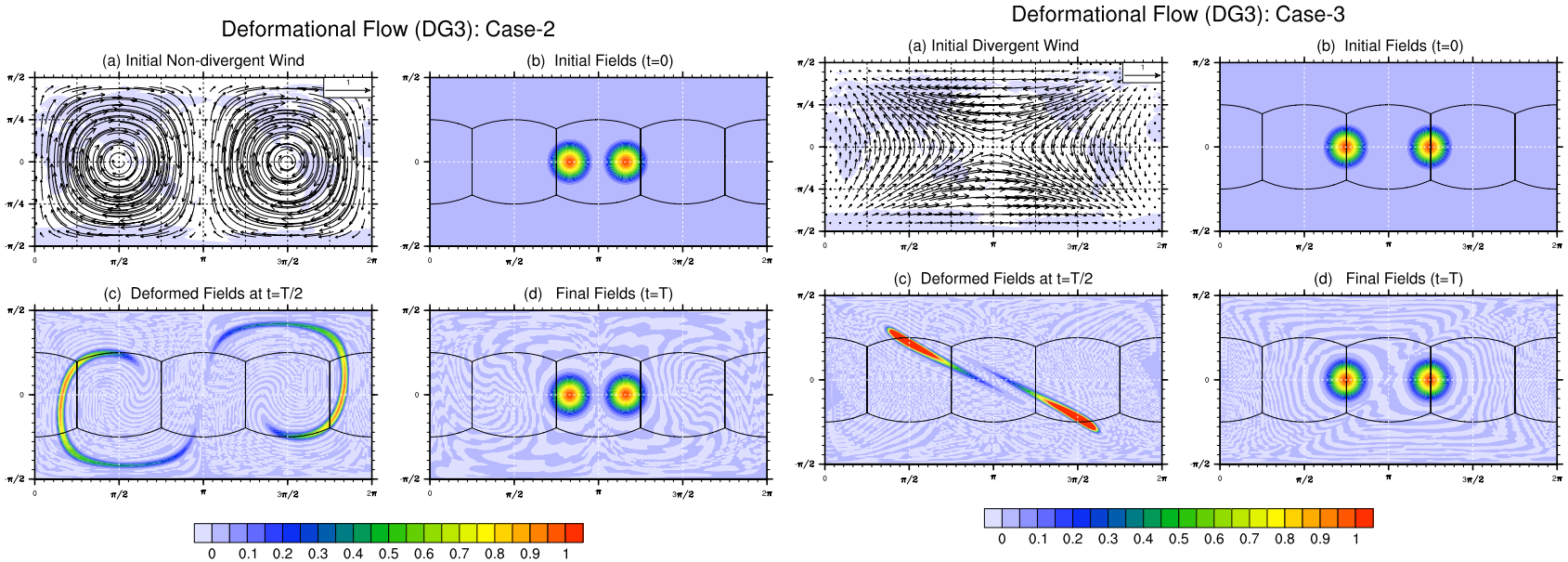

- Note: You can use any spatial distribution as the initial condition
- At DOE transport meeting 3 weeks ago it was suggested to add solid-body rotation to the flow (to avoid the possibility of cancellation of errors when the flow reverses)
- Also: Shifted initial condition (if tracer q is zero it can hide some artifacts ...)
- Show animations ...

Class of deformational test cases (Nair and Lauritzen 2010, in review)

- Test forces modelers who transport tracer mass and not q to distinguish between density and concentration (even for the non-divergent flow no scheme will preserve a constant!)
- Very challenging flow conditions
- Test can, of course, be rotated to direct flow over your 'trouble points'
- This test can be setup to test accuracy of sub-cycling (smooth background air mass field and non-smooth tracer field)

Class of deformational test cases (Nair and Lauritzen 2010, in review)

- (as part of DOE transport efforts) We plan to organize a short working workshop at NCAR in early 2011
  - Participants must bring solutions!
  - A draft test case setup will be formulated later this year (goal: get at accuracy versus cost, gradient preservation, accuracy and cost of filters/limiters, ...)
  - Comments are very welcome! (perhaps add simplified chemistry, L.Bonaventura)

Questions

References I

Barth, T. and Jespersen, D. (1989). The design and application of upwind schemes on unstructured meshes. *Proc. AIAA 27th Aerospace Sciences Meeting, Reno*.

Blossey, P. and Durran, D. (2008). Selective monotonicity preservation in scalar advection. *J. Comput. Phys.*, 227(10):5160–5183.

Dukowicz, J. K. and Baumgardner, J. R. (2000). Incremental remapping as a transport/advection algorithm. *J. Comput. Phys.*, 160:318–335.

Harris, L. M. and Lauritzen, P. H. (2010). A flux-form version of the conservative semi-lagrangian multi-tracer transport scheme (cslam) on the cubed sphere grid. *J. Comput. Phys.* submitted.

Lauritzen, P., Jablonowski, C., Taylor, M., and Nair, R. (2010a). Rotated versions of the jablonowski steady-state and baroclinic wave test cases: A dynamical core intercomparison. *Journal of Advances in Modeling Earth Systems*. in press.

Lauritzen, P. H., Nair, R. D., and Ullrich, P. A. (2010b). A conservative semi-Lagrangian multi-tracer transport scheme (cslam) on the cubed-sphere grid. *J. Comput. Phys.*, 229:1401–1424.

LeVeque, R. (1996). High-resolution conservative algorithms for advection in incompressible flow. *SIAM J. Numer. Anal.*, 33:627–665.

Nair, R. and Lauritzen, P. H. (2010). A class of deformational flow test-cases for the advection problems on the sphere. *J. Comput. Phys.* submitted.

Nair, R. D. and Jablonowski, C. (2008). Moving vortices on the sphere: A test case for horizontal advection problems. *Mon. Wea. Rev.*, 136:699–711.

Putman, W. M. and Lin, S.-J. (2007). Finite-volume transport on various cubed-sphere grids. *J. Comput. Phys.*, 227(1):55–78.

Sadourny, R. (1972). Conservative finite-difference approximations of the primitive equations on quasi-uniform spherical grids. *Mon. Wea. Rev.*, 100:136–144.

Ullrich, P. A., Lauritzen, P. H., and Jablonowski, C. (2009). Geometrically exact conservative remapping (GECoRe): Regular latitude-longitude and cubed-sphere grids. *Mon. Wea. Rev.*, 137(6):1721–1741.

Zalesak, S. T. (1979). Fully multidimensional flux-corrected transport algorithms for fluids. *J. Comput. Phys.*, 31:335–362.